



Univerzita Komenského v Bratislave

Fakulta matematiky, fyziky a informatiky



**Mgr. Branislav Pongráč**

Autoreferát dizertačnej práce

**Study of the Electro spraying Effect of Water in Combination  
with Atmospheric Pressure Corona Discharge**

na získanie akademického titulu: **philosophiae doctor**

v odbore doktorandského štúdia: **4.1.6. Fyzika plazmy**

**Bratislava 2014**

Dizertačná práca bola vypracovaná v dennej forme doktorandského štúdia na Katedre astronómie, fyziky Zeme a meteorológie, Fakulty matematiky, fyziky a informatiky Univerzity Komenského v Bratislave.

**Predkladateľ:**     **Mgr. Branislav Pongráč**  
Katedra astronómie, fyziky Zeme a meteorológie, Fakulta matematiky, fyziky a informatiky  
Univerzita Komenského  
Mlynská Dolina, 842 48 Bratislava 4

**Školiteľ:**           **Doc. RNDr. Zdenko Machala, PhD.**  
Katedra astronómie, fyziky Zeme a meteorológie, Fakulta matematiky, fyziky a informatiky  
Univerzita Komenského  
Mlynská Dolina, 842 48 Bratislava 4

**Oponenti:**           .....  
.....  
.....  
.....

**Doc. RNDr. František Krčma, PhD.**  
Ústav fyzikálnej a spotrebnej chémie, Fakulta chemická  
Vysoké Učenie Technické  
Purkyňova 118, Královo Pole, 612 00 Brno, Česká republika

.....  
.....  
.....  
.....

Obhajoba dizertačnej práce sa koná ..... o ..... h  
pred komisiou pre obhajobu dizertačnej práce v odbore doktorandského štúdia vymenovanou predsedom  
odborovej komisie .....,

v študijnom odbore **4.1.6. Fyzika plazmy,**

na **Fakulte matematiky, fyziky a informatiky Univerzity Komenského, Mlynská Dolina, 842 48 Bratislava.**

Predseda odborovej komisie:  
**Prof. RNDr. Štefan Matejčík, DrSc.**  
Katedra experimentálnej fyziky, Fakulta matematiky, fyziky a informatiky  
Univerzita Komenského  
Mlynská Dolina, 842 48 Bratislava 4

## Abstract

This thesis explores the effect of electro spraying (EHDA) of water in combination with atmospheric positive DC corona discharge. The electro spraying effect of liquids has been a subject of research since the beginning of the last century and found importance in many diverse fields. Recently, one of the potential uses of water electro spray, especially large flow rate modes, has become a decontamination of water from organic and microbial pollutants. The presence of an electrical discharge generating non-thermal plasma in the spraying zone allows for very efficient mass transfer of plasma-generated species into water. We used a point-to-plane geometry of electrodes with a various types of hollow syringe needle anodes opposite to the metal mesh cathode. We employed mainly the iCCD and high-speed (HS) camera visualization techniques, oscilloscopic discharge current measurements and total average current measurements, and optical emission spectroscopy (OES). These were used in order to visualize the formation of water jets (filaments) in various electro spraying modes and to investigate the corona discharge behavior during this process. The following modes of electro spraying typical for water were observed: dripping mode and spindle modes for low and medium flow rates, and simple jet modes for high flow rates. The geometry of HV stressed electrodes had a significant influence on the electro spraying process. Nozzle was more suitable for stable electro spray generation and needle for intense discharge generation. We observed different electro spraying behavior in dependence on the water flow rate and water conductivity. Also the corona discharge behavior was influenced by these parameters. Generally, pointy, elongated, and fast spreading water filaments were observed for lower conductivity; in contrast to rounder, broader, and shorter quickly disintegrating filaments for higher conductivity. In addition, with increasing conductivity, the breakdown voltage for corona-to-spark transition was decreasing. For limited range of voltages, the frequency of intermittent water filament generation in spindle modes agreed well with the frequency of the measured streamer current pulses. After each streamer, a positive glow corona discharge was established on the water filament tip and it propagated from the stressed electrode along with the water filament elongation. These results show a reciprocal character of intermittent electro spraying of water and the presence of corona discharge, where both the electro spray and the discharge affect each other.

**Keywords—**Electrospray, DC corona discharge, bio-decontamination, high-speed camera, iCCD imaging

# 1 Introduction

## 1.1 Background and motivation

The electro spraying effect of liquids has been a subject of research for more than a century. The pioneering works conducted by [1,2] were among the first published experimental studies in this field, followed by others. Another important study was conducted by Taylor who first derived the condition for stable liquid cone existence [3]. Since then, the electro spray became the subject of extensive studies by many researchers [4–11]. It found importance in such diverse fields as thin film deposition, drug inhalation, spray painting and surface coating, ink-jet printers or as a source of ions of macromolecules for mass spectrometry among many others.

The electro spraying effect can be generally explained as follows. When the liquid medium (in our case water) flowing through the capillary (or nozzle) is not subjected to electrical stress, regular droplets with rounded shapes are formed from the end of the capillary. In this situation, the droplet size is given by the balance of capillary and gravitational forces. However, with application of an electrical potential on the capillary, electric forces take effect. The effective surface tension of the liquid starts to decrease due to the presence of the electric field causing the charge separation inside the liquid and the volume of the forming droplets decreases. The charges of the polarity of the capillary move towards the droplet surface and induce a surface charge density, causing an increase of the electrostatic pressure against the capillary pressure. When a critical voltage is reached, the shape of the droplet changes into conical, which is referred to as Taylor cone [3]. Under these conditions, there has to be a hydrostatic balance between the capillary pressure and the normal electric pressure at the conical surface of the liquid. Subsequently, a jet emerges from the tip of the Taylor cone and breaks into droplets due to the axisymmetric (varicose), lateral (kink), or ramified instabilities [12]. These charged droplets are then accelerated by the electric field; Coulomb repulsion takes effect between them and finally the electro spray occurs. During the electro spray, the size of the droplets can vary from tens of nm up to hundreds of  $\mu\text{m}$  [13,14].

The electro spraying effect of water in combination with an atmospheric plasma discharge can lead to a potential application; decontamination of water polluted with organic and microbial pollutants. In such case, the water flows directly through the high-voltage (HV) needle electrode into the active discharge region, where it is sprayed into small droplets. The presence of the electrical discharge generating non-thermal plasma in the spraying area allows for very efficient mass transfer of plasma-generated species into water.

Moreover, electrical discharges in combination with electro sprayed droplets have not been fully understood. In this regard, it is necessary to better investigate the effect of electro spraying in combination with the discharge under various conditions.

## 1.2 Objectives of the work

- (i) **To study and identify the electro spraying modes of water observed during investigation of corona discharge in combination with electro spraying.**

Various modes of water electro spraying occurred in our measurements with corona discharge were investigated and identified in accordance with the literature. For this purpose we used mainly high-speed camera visualization. The advantage of this method is a time-resolved visualization of fast phenomena that are normally very hard to detect by naked eye or standard digital camera with low frame rate.

**(ii) To study the influence of water with various flow rates on the electro spray with corona discharge.**

The effect of electro sprayed water and its flow rate on the discharge behavior was investigated for various stressed electrodes. The presence of water cone can influence the discharge generation. For this purpose we used the I-V measurements and photo documentation.

**(iii) To study the influence of water conductivity on the electro spray with corona discharge.**

The effect of water conductivity on the particular electro spray modes in combination with positive DC corona discharge was investigated. Our main objective was to investigate and explain the spray behavior and especially the water filament (water jet) formation in dependence on the water conductivity. The discharge generation and its behavior during this process of electro spraying were also investigated. For this purpose we used high-speed camera visualization, I-V measurements with optical emission spectroscopy, and photo documentation.

**(iv) To study the mutual influence of the corona discharge and the electro spray.**

The current pulses occurred during the measurements were investigated and identified in relation with the electro spray. Additionally, the mutual influence of the corona discharge and water electro spraying were observed and studied considering the electric field distortion and ionic space charge effects. We used the high-speed camera measurements supplemented with the records of the discharge generation and propagation during the electro spray process by iCCD camera, photomultiplier tube responses, and oscilloscopic current measurements of discharge.

**(v) To summarize the results considering the potential effects in bio-decontamination.**

## 2 Experimental set-up

Owing to the diversity of parameters involved in electro spraying of liquids, it is necessary to limit the field of investigations. We shall consider here only the case of a vertical metallic electrode (capillary), brought to a positive voltage and supplied with liquid at a constant flow rate. Capillaries of different geometries were used during the experiments. We used only water with various conductivities as the electro sprayed liquid.

The experiments were conducted in air at ambient temperatures of about 20-25 °C.

During the study of the electro spraying phenomena with the presence of the discharge we used a complex experimental set-up consisting of various experimental devices and methods. The complex scheme of this set-up is shown in Fig. 1.

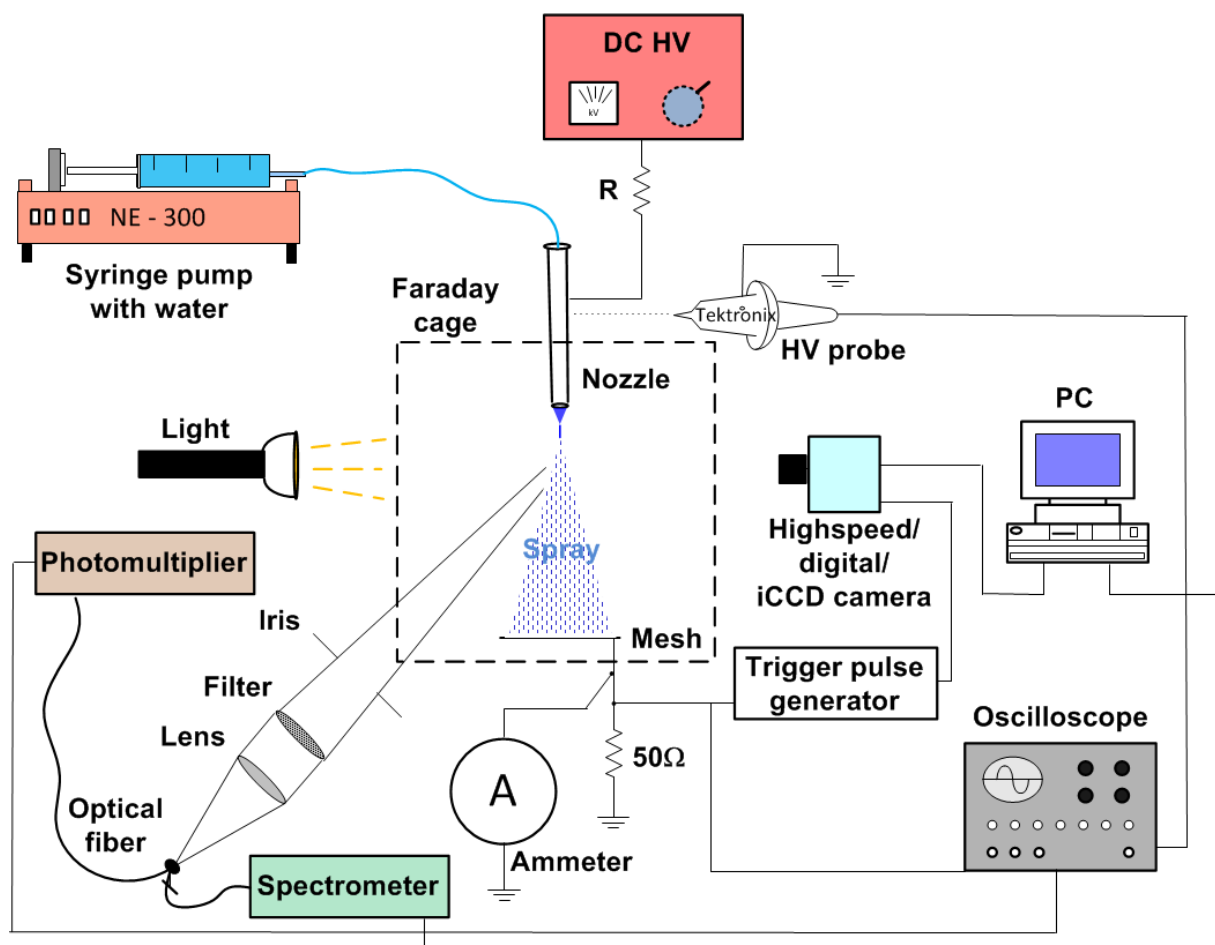


**Fig. 1** Experimental set-up for investigations of electro spray of water, with a high-voltage hollow needle (nozzle) electrode enabling water flow into the inter-electrode space.

### **3 Identification of the observed electrospaying modes**

In our experimental set-up with using water as the electrospayed liquid, we observed a typical behavior of droplet formation at the tip of the nozzle and its deformation with the applied electric field. Only limited number of modes of electrospaying was observed and identified in our configuration. The corona discharge was present from the very beginning of the electrospray due to the high surface tension of water. Consequently, stable cone-jet modes were not established because the field required exceeded that for the electric breakdown in the gas surrounding the cone [4,15,16]. Additionally, for our range of conductivities, the flow rates were probably out of the range for stable cone-jet electrospaying. According to [8] the maximum flow rates for liquids with conductivities  $0.03 \mu\text{S}/\text{cm}$  and  $0.36 \mu\text{S}/\text{cm}$  are approximately  $0.06 \text{ ml}/\text{min}$  and  $0.018 \text{ ml}/\text{min}$ , respectively. For conductivities used in this work the extrapolated flow rate values would lay significantly under our used flow rates.

Microdripping mode was not observed probably due to the relatively high flow rates.

For recording of the fast electrospaying phenomena we used the high-speed camera imaging.

The summary of these observations can be seen in Tab. 1.

**Tab. 1 High-speed camera images of the electrospray of water with 3 different conductivities and flow rates (nozzle 0.5 mm i.d., 0.7 mm o.d., gap 5 cm, positive DC).**

| $K_1 = 2 \mu\text{S/cm}$    |  | $K_2 = 400 \mu\text{S/cm}$              |   | $K_3 = 4000 \mu\text{S/cm}$ |                                 |
|-----------------------------|--|---|---|-----------------------------|---------------------------------|
| $Q_1 = 0.04 \text{ ml/min}$ | 7-9 kV<br>intermitt. cone-jet          | 10-12 kV<br>spindle+intermitt. cone-jet | 13<kV<br>spindle                                | 6-9 kV<br>dripping          | 10-12 kV<br>spindle             |
| $Q_2 = 0.4 \text{ ml/min}$  | 7-8 kV<br>dripping+intermitt. cone-jet | 9-12 kV<br>spindle+intermitt. cone-jet  | 13-14 kV<br>spindle                             | 7-9 kV<br>dripping          | 10-12 kV<br>dripping+spindle    |
| $Q_3 = 4 \text{ ml/min}$    | 8-9 kV<br>simple-jet                   | 10-19 kV<br>simple-jet/oscill. jet      | 20<kV<br>simple-jet/rotating jet                | 7-10 kV<br>simple-jet       | 11<kV<br>simple-jet/oscill. jet |
| $Q_1 = 0.04 \text{ ml/min}$ | 13<kV<br>spindle                       | 15-16 kV<br>oscill. spindle             | 17-19 kV<br>oscill. spindle+intermitt. cone-jet | 8-12 kV<br>spindle          | 13-17 kV<br>dripping/spindle    |
| $Q_2 = 0.4 \text{ ml/min}$  | 7-9 kV<br>dripping                     | 10-12 kV<br>spindle                     | 13-17 kV<br>dripping/spindle                    | 7-9 kV<br>dripping          | 10-12 kV<br>dripping+spindle    |
| $Q_3 = 4 \text{ ml/min}$    | 7-9 kV<br>simple-jet                   | 10<kV<br>simple-jet/oscill. jet         | 10<kV<br>simple-jet/oscill. jet                 | 7-10 kV<br>simple-jet       | 11<kV<br>simple-jet/oscill. jet |
| $Q_1 = 0.04 \text{ ml/min}$ | 13<kV<br>dripping/oscill. dripping     | 13<kV<br>dripping/oscill. dripping      | 18<kV<br>oscill. dripping                       | 13<kV<br>dripping/spindle   | 18<kV<br>oscill. dripping       |



## 4 Influence of the water electrospray on the corona discharge

The effect of intermittent electrospraying of water similar to the spindle and oscillating spindle mode was studied in combination with DC streamer corona discharge under various voltages and water flow rates.

We observed differences in the dependence of electrospraying on the applied voltage and water flow rates. Fig. 2 shows the comparison of three different flow rates (0.05, 0.5 and 1.5 ml/min for rows 1, 2 and 3, respectively) at three different voltages (6, 7 and 8 kV). For each voltage and flow rate, we present a pair of photographs showing the water stream (illuminated) and the discharge region (dark) under the same conditions, together with the average streamer current pulse and frequency of these pulses.

Without water, the corona discharge is very stable. Therefore, we expected the best stable spraying conditions at low water flow rates. However, at low flow rate (0.05 ml/min; see upper row in Fig. 2), the streamer corona was relatively intense but not too stable and sometimes was altered from side to side by the flow. Spraying was also unstable; we observed erratic water streams from the electrode probably because of the insufficient water supply. This erratic behavior of the electrospraying could influence the behavior of the discharge, and caused some irregularities in the discharge geometry pattern. The discharge with high intensity is created only from the one side of the electrode.

The best conditions with a good stability and intensity of the streamer corona with a relatively stable electrospraying in its active region were reached for medium flow rate (0.5 ml/min; see middle row in Fig. 2). In this case the discharge with high intensity is created from the both sides of the electrode, thus creating the regular discharge geometry pattern. With the increasing voltage, the dispersion of the spray increased because the water droplets with similar charges stronger repelled one another, and also due to the higher amplitudes of water filament oscillations.

At high flow rates (1.5 ml/min; see bottom row in Fig. 2), the formation of streamer corona was too much disrupted and eventually quenched by the water flow. In addition, the electrical breakdown occurred at lower voltage than at lower flow rates. It looks like the streamer corona is prevented to occur from the sharp tips of the needle, but is more likely to occur from the water filament.

This is an interesting and important conclusion for the next research and water decontamination applications.

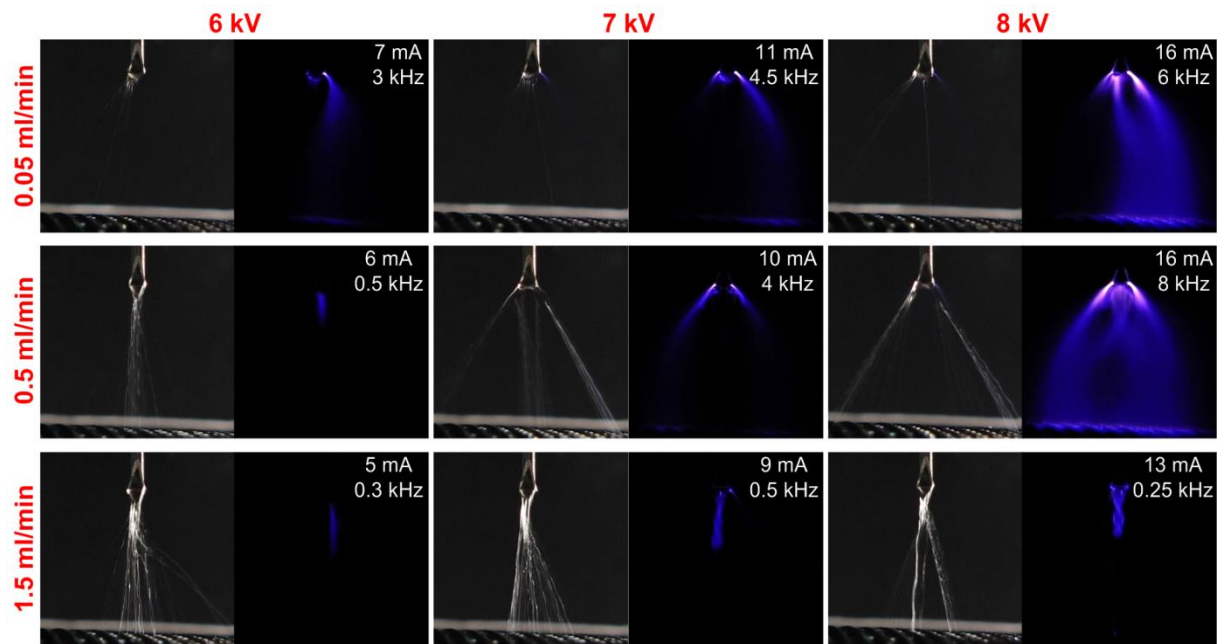


**Fig. 2** Electrospaying effect with streamer corona discharge depending on the voltage and the water flow rate with the typical current amplitudes and frequencies (modified needle, 1 cm gap, f/2.7). Exposure time was 1/15 s for illuminated pictures showing water streams and 4 s for dark pictures showing discharge regions under the same conditions.

## 5 Influence of the water conductivity on electrospray with discharge

### 5.1 Influence of the water conductivity on the electrospray

Conductivity of the liquid is a significant parameter that influences the electrospray and its behavior. When the liquid has a relatively low conductivity, an electric potential difference between the base (end) of the capillary (nozzle) and the end of the liquid filament can exist. This potential drop ensures that the liquid–air interface is subjected to a tangential electric field  $E_t$  and a tangential electrical shear stress in the direction of the flow [17,5,6,18]. For high conductivity liquids, such as regular tap water (400-500  $\mu\text{S}/\text{cm}$ ); the liquid surface can be almost equipotential. Although the surface is charged, it is not subjected to a significant tangential electric field and a tangential electric shear stress. Instead, it is subjected to a normal electric field and a normal stress which tends to destabilize the propagating water filament or a jet [5].

In dependence on the water conductivity we observed different filament shapes and behaviors. In the first set of measurements (Fig. 3 and Fig. 4) with the parameters (gap 5 cm, water flow rate 0.4 ml/min, voltage +11 kV), no permanent jet occurred. The jet was just periodically forming from the cone tip by its elongation and was subsequently tearing off from the water meniscus as a thin liquid filament. This is described in the literature as a spindle mode of electrospaying [15,19].

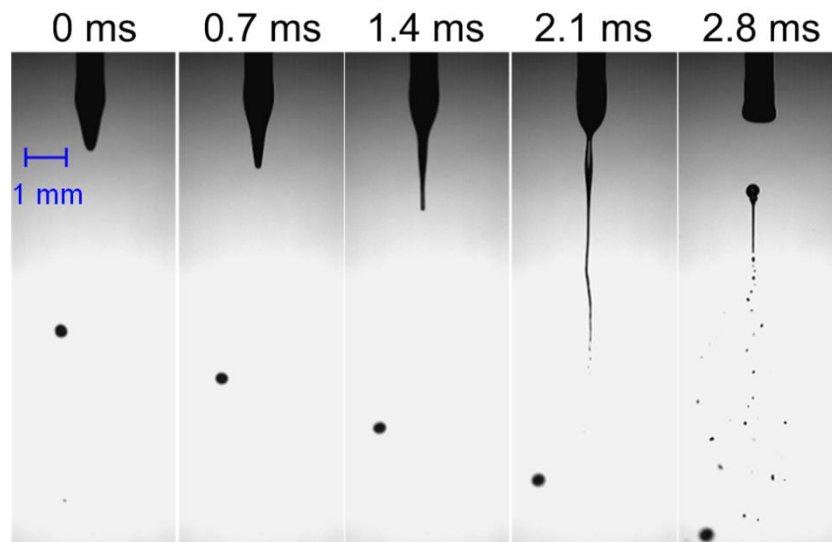


**Fig. 3 High-speed camera sequence of the spindle mode electrospray with low conductivity 2  $\mu\text{S}/\text{cm}$  water (10 000 fps, 1  $\mu\text{s}$  gate time, time step 700  $\mu\text{s}$ , flow rate 0.4 ml/min, voltage +11 kV, nozzle 0.5 mm i.d., 0.7 mm o.d., 5 cm gap).**

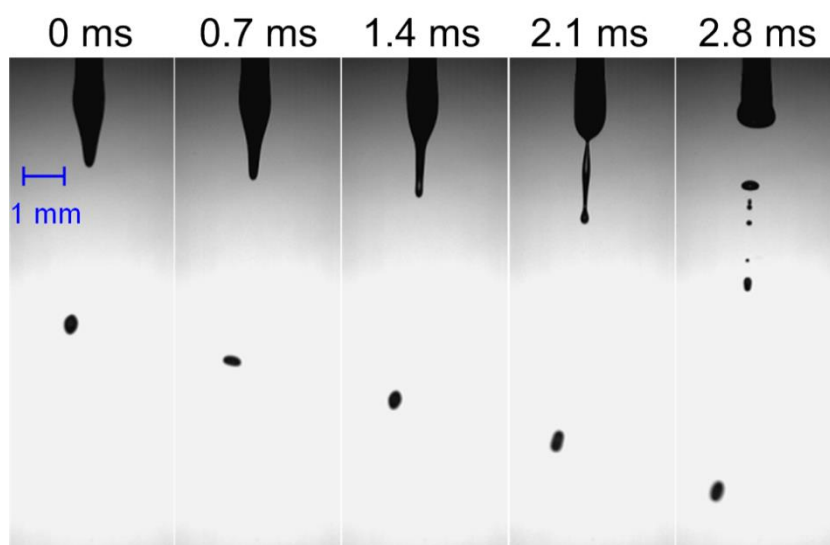


**Fig. 4 High-speed camera sequence of the spindle mode electrospay with high conductivity 400  $\mu\text{S}/\text{cm}$  water (10 000 fps, 1  $\mu\text{s}$  gate time, time step 700  $\mu\text{s}$ , flow rate 0.4 ml/min, voltage +11 kV, nozzle 0.5 mm i.d., 0.7 mm o.d., 5 cm gap).**

After this detachment, the filament disintegrated into small droplets under the action of surface tension forces and the water meniscus shrank back to the nozzle. In Fig. 3, deionized water with conductivity 2  $\mu\text{S}/\text{cm}$  was used, which is much lower than 400  $\mu\text{S}/\text{cm}$  shown in Fig. 4. Both image sequences were taken starting right after the cone creation at the end of the nozzle until the detachment of the water filament from the main water meniscus and its following disintegration. In both Figs., the time step between single images was 700  $\mu\text{s}$ . It can be seen that with 2  $\mu\text{S}/\text{cm}$  conductivity (Fig. 3), the water filament is of significantly different shape, more elongated and thinner at the filament head, in comparison with 400  $\mu\text{S}/\text{cm}$  (Fig. 4), where the filament is shorter with the rounded thicker filament head. Because the size of droplets is directly proportional to the diameter of the filament, low conductivity water (2  $\mu\text{S}/\text{cm}$ ) produced smaller droplets than the high conductivity water (400  $\mu\text{S}/\text{cm}$ ).

With a closer look at Fig. 3 and Fig. 4, the parts of the filaments under the nozzle (~2 mm from the nozzle) are similar for both conductivities; however the bottom parts (i.e. the filament heads) are significantly different. This different shape can be due to the discharge presence in the proximity of water surface.

With a close examination of previous Figs. we can notice that the velocity of water filament head propagation strongly depends on the conductivity. Because both image sequences were recorded by the high-speed camera with the same time step, we were able to calculate the velocity of water filament propagation, as shown in Fig. 5. The velocity was calculated for a number of points as a difference of water filament lengths over exact times, until the water filament detached from the nozzle. The velocity-time curves are divided into two main areas: the slower area with lower propagation velocities (in Fig. 5 from 0 to 3 ms, marked as Cone forming period), where the cone is still forming and starts to transform into filament, and the faster area with higher propagation velocities (in Fig. 5 from 3 ms higher, marked as filament propagation), where the filament is propagating towards the ground electrode until its disintegration. One can see that for the lower conductivity (blue triangles), the velocity-time curve is more exponential in comparison with higher conductivity (green circles). It means

that the acceleration and probably the acting force are higher too, as can be seen from the calculated acceleration values in Fig. 5.

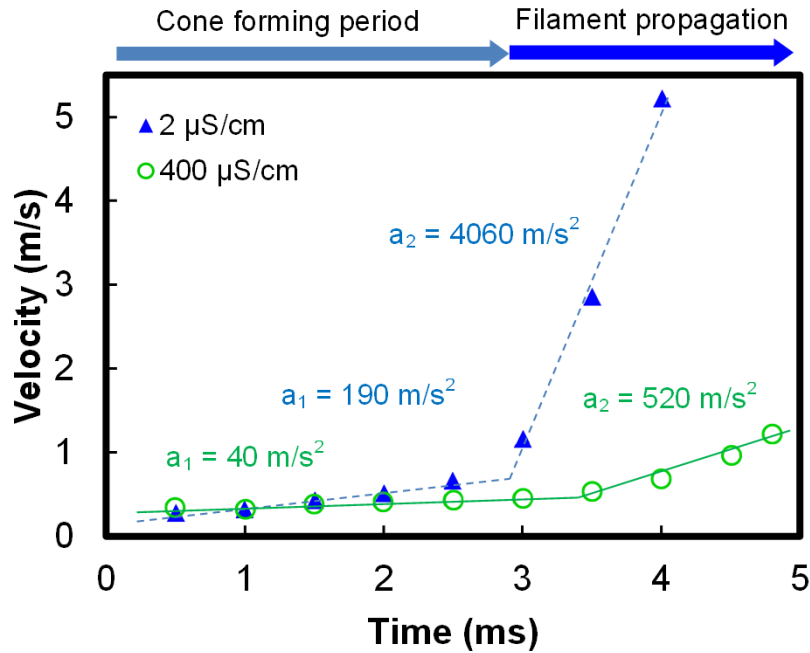


**Fig. 5 Comparison of water filament velocities during the cone formation and filament propagation of the spindle mode for 2 different conductivities (spindle mode, flow rate 0.4 ml/min, voltage +11 kV, nozzle 0.5 mm i.d., 0.7 mm o.d., 5 cm gap).**

This is very likely caused by the effect of different tangential electric fields and resultant tangential electric forces mentioned above. In addition, the rates of acceleration in the filament front during the filament propagation period were 4060 m/s<sup>2</sup> and 520 m/s<sup>2</sup> for 2 μS/cm and 400 μS/cm, respectively, which are greatly far above the gravitational acceleration (9.8 m/s<sup>2</sup>). This clearly indicates that the process is mainly governed by the electrostatic force and the gravitational force can be neglected.

## 5.2 Influence of the water conductivity on the discharge properties

In the first set of measurements we used the nozzle HV electrode. We detected the corona discharge starting from about 6 kV in 2 cm gaps.

Interesting results are demonstrated in Fig. 6 for 2 cm gap distance. With the increasing voltage, the total average current values were measured for 3 different water conductivities: 290; 2900; and 29,000 μS/cm. Measurement was carried out from the lowest current values until the sparking occurred. Subsequently, I-V characteristics were plotted. As can be seen in Fig. 6 for 2 cm gap, when the conductivity is increasing, the breakdown voltage for corona-to-spark transition is decreasing. The breakdown voltage corresponds to the maximum possible corona voltage before the sparking occurs.

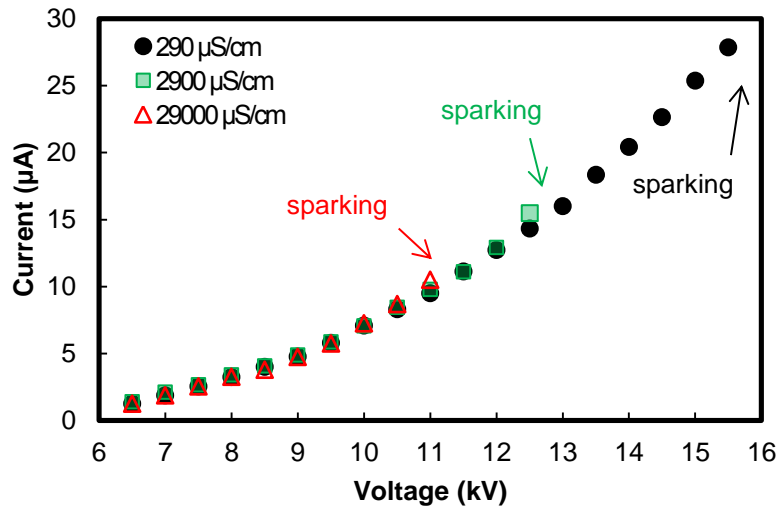


**Fig. 6 I-V curves for electro spraying of water with corona discharge (spindle modes, 2 cm gap, nozzle 0.6 mm i.d., 0.8 mm o.d., flow rate 0.4 ml/min). Different breakdown voltages for corona-to-spark transition are due to different conductivity effect.**

Considering the spray behavior shown in Fig. 3 and Fig. 4, this phenomenon can be explained as follows: since the highly conductive liquid acts as a relatively good conductor, the voltage drop on the filament is negligible and the electric field should be stronger on the highly conductive water meniscus. The discharge is thus permitted to occur at the liquid surface and the discharge activity on the water filament tip is then enhanced as the filament proceeds toward the ground electrode and reduces the effective gap distance. For better understanding, this process is similar to the reduction of gap distance by shifting the position of the HV needle electrode towards the ground electrode. During this process, the filamentary streamer discharge can occur from the tip through the entire gap space which can eventually facilitate the spark generation at a relatively low voltage. On the other hand, for poorly conductive liquids, the liquid acts more as an insulator and the voltage drop on the filament is more significant as in the case of conducting liquid. Additionally, the electrical resistance of the growing water filament increases with the filament length and suppresses the corona activity on its surface. Therefore, the corona space charge is prevented from accumulating on the propagated filament surface and so the discharge can be also forced to occur more easily on the metal electrode. Subsequently, the spark does not occur until the higher voltage [17,20].

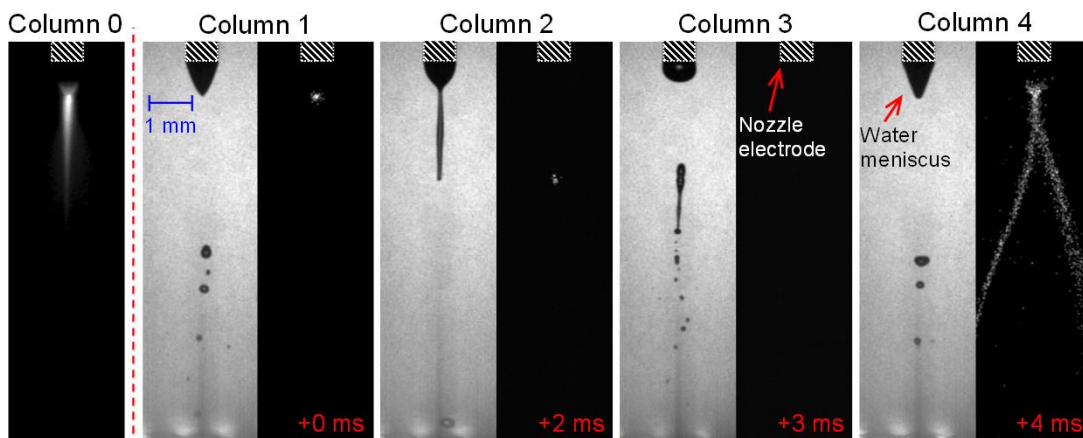
## 6 Investigation of corona discharge during the electrospaying in spindle mode

### 6.1 iCCD imaging procedure

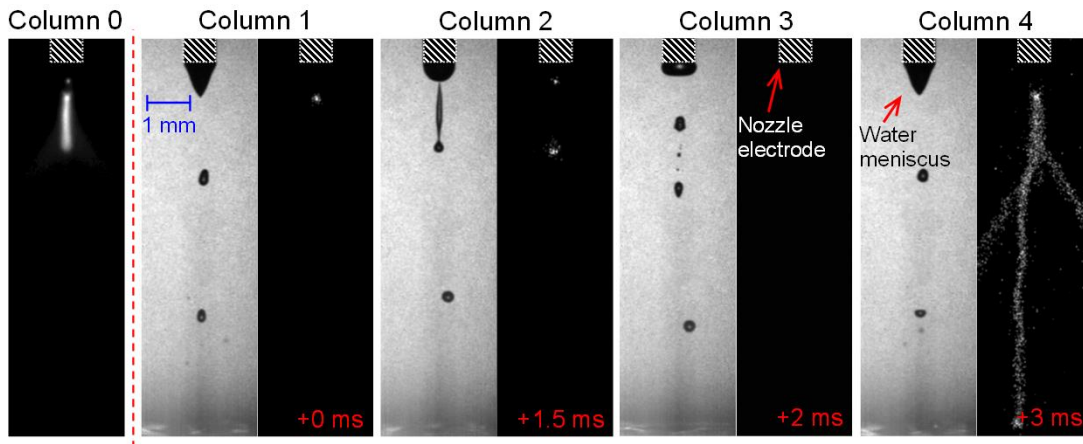
In these measurements we used the iCCD camera that was triggered by the discharge current pulse.

Fig. 7 and Fig. 8 show the iCCD images of spindle modes at voltage 6 kV using 2 different conductivities ( $4 \mu\text{S}/\text{cm}$  and  $500 \mu\text{S}/\text{cm}$ ), respectively. For each illuminated image with droplets, the corresponding dark image of the discharge emission without illumination is shown. During these measurements, the gain function (related to light intensification) of the iCCD camera was adjusted differently for illuminated and dark images to reach a proper visualization. The exposure time was  $10 \mu\text{s}$  for the illuminated (no light intensification) and  $100 \mu\text{s}$  for the dark images (maximum light intensification), respectively. The only exception is the left column 0 with dark images where the exposure time was 5 s (no light intensification), representing an integrated emission over the long period with many droplet formation cycles.

The camera delay was gradually increased to the point when the image was approximately the same as the first one in the sequence (the droplet was at the same position). At this point, the next electrospaying event starts (column 4). These images represent different stages of the electrospaying event and the discharge propagation from 0 to 3, and 4 ms (columns 1-4).



**Fig. 7** iCCD time sequence images of electrospaying of water (illuminated, exposure time  $10 \mu\text{s}$ ) with corona discharge (dark, exposure time  $100 \mu\text{s}$ ), conductivity  $4 \mu\text{S}/\text{cm}$ , + 6 kV, gap 1 cm, column 0 with exposure time 5 s represent an integrated emission over the long period.



**Fig. 8** iCCD time sequence images of electro spraying of water (illuminated, exposure time  $10\ \mu\text{s}$ ) with corona discharge (dark, exposure time  $100\ \mu\text{s}$ ), conductivity  $500\ \mu\text{S}/\text{cm}$ ,  $+6\ \text{kV}$ , gap  $1\ \text{cm}$ , column 0 with exposure time  $5\ \text{s}$  represent an integrated emission over the long period.

## 6.2 Propagation of corona discharge during the electro spray and their mutual influence

Thanks to the combined sequences in previous figures it is possible to see the propagation of the discharge in relation with the water cone formation and propagation. For all 2 conductivities shown, the glow corona is first visible at the tip of the water cone (column 1). The water cone gradually elongates and creates the filament. As the water filament propagates axially towards the grounded electrode, the bright spot of the glow corona remains present at the tip of this filament and propagates with it (column 2).

Although intuitively expected, we did not observe any corona discharge originating directly from the nozzle in the range of the studied (pre-breakdown) voltages ( $4.5\text{--}7\ \text{kV}$ ) in  $1\ \text{cm}$  gap. This is demonstrated in Fig. 7 and Fig. 8, too, where the edges of the nozzle are shown with no light emission. Unlike in some other bio-decontamination studies of our group [21,22], the nozzle used here was a blunt hollow needle and so higher voltages would be needed to initiate the corona discharge on its edges. On the contrary, sequences of dark images in Fig. 7 and Fig. 8, as well as the integrated emission in column 0 clearly demonstrate light emission of the glow corona discharge at the tip of the Taylor cone and the propagating water filament, eventually terminated with a filamentary discharge occurring in each cycle of the droplet formation.

We observed the glow corona originating from the pointed filament tip even for the lowest water conductivities, despite the filament of water of such low conductivity represents a significant electrical resistance (as much as  $5\ \text{M}\Omega$  for  $\sim 1\ \text{mm}$  long Taylor cone of  $4\ \mu\text{S}/\text{cm}$  water seen in Fig. 7, column 1, and as much as  $55\ \text{M}\Omega$  for  $\sim 2.8\ \text{mm}$  elongated thin filament seen in Fig. 7, column 2). The electrical resistances of water filaments were estimated by using the Pouillet's law.

However, the currents in the glow corona regime are low ( $\sim\mu\text{A}$ ), so the voltage drop across the filament remains too low to completely suppress the enhancement of the electric field around the tip and formation of the corona ( $\sim 10\ \text{V}$  in Fig. 7, column 1; up to max  $150\ \text{V}$  in the



most extreme case in Fig. 7, column 2). The voltage drops across water filaments were estimated by using the Ohm's law.

The appearance of corona on the water filament tip is primarily the electric field effect. However, a closer look at this tip indicates how the ionic space charge resulting from the corona seems to affect the surface electric field at the filament and the shape of its tip (Fig. 7 and Fig. 8, illuminated images in column 2). The similar effect was observed and described by [17,13]. In highly conductive liquids, the liquid acts as a conductor and does not impose a significant voltage drop. The discharge activity on the filament tip and its resultant space charge around the tip are therefore enhanced as the liquid filament proceeds along the gap. Since the filament head with active corona is surrounded by a strong space charge of ions of the same polarity, the electric field and so the electric pressure on the filament head become more reduced. Under such conditions, the capillary pressure also decreases to equilibrate the reduced electric pressure and the tip thus becomes more spherical with a surface of larger radius of curvature [17].

On the other hand, in poorly conductive liquids the liquid acts more as insulator and so the electrical resistance of the growing water filament partially suppresses the corona activity. Therefore, the corona ionic space charge is prevented from accumulating near the filament surface, and subsequently the surface electric field of the filament tip is not reduced as much as in the conductive liquids. Therefore, the tip is more pointed with a surface of smaller radius of curvature [17].

After the detachment of the elongated water fragment and the contraction of the water meniscus back towards the nozzle, the glow corona disappeared (column 3, the dark image is without any bright spots). This may be simply caused by the reduction of the electric field near the nozzle due to the decrease in the water meniscus curvature simply due to insufficient water volume to form the cone. Additionally, the presence of the droplets under the nozzle could also reduce the field, since they carry charges of the same polarity as the nozzle and weaken the field on it [19,12]. With the disappearance of corona activity on the meniscus surface, the surface electric field is no longer reduced by the corona space charge and so the enhanced electric field on the water surface of the newly accumulated water droplet starts to deform its surface again, thus reforming a cone.

Finally, after a few ms, a new cone is formed (decreasing the radius of curvature and so increasing the intensity of the electric field), and the filamentary discharge occurs from the cone tip to the ground electrode (column 4). This discharge is similar to the onset streamer in short gaps and is responsible for the generation of the measured current pulses that trigger the iCCD camera.

The electro spraying event with discharge propagation did not change very much with increasing the voltage within the studied range. However, with higher voltage, the glow corona was always present on the water meniscus even after the detachment of elongated water fragment from the nozzle. This led to the formation of the water cone that was not as sharp as with the lower voltage shown in columns 1 and 4 of Fig. 7 and Fig. 8, but was more rounded. A filamentary discharge eventually occurred from this rounded cone, too.

According to the theory of the streamer and glow corona generation from metal surface extensively elaborated and described elsewhere, e.g. in [23,24], the onset streamer is always present before the start of a positive glow corona. Obviously, the same phenomenon can be

observed in the experiment with electrospray. The difference in our case is that the surface is a liquid and it oscillates. Thus, this corona discharge is unstable and depends on the water meniscus propagation. On the other hand, the presence of a discharge generating a space charge in the vicinity of water meniscus causes the reduction of the electric field in this area. This can disrupt the balance between the electric and the capillary forces determining the water filament shape, propagation, and stability [17,8].

These results show the reciprocal character of intermittent electrospraying of water with the presence of corona discharge, where both phenomena affect each other.

## Summary

In this work we aimed to investigate the combined effect of corona discharge with electrospray to provide knowledge about possibilities of use this method as a potential application for bio-decontamination of water. However it is important to note that this work was not directly focused on the application, thus no results dealing with the applications are presented.

Additionally, we aimed to contribute to the fundamental understanding of electrical discharges in electrospraying process. Although our results cannot be considered as conclusive ones, they certainly provide interesting data dealing with electrical discharges in electrospraying process.

In accordance with the objectives of the work we can summarize the main conclusions of our work.

### **(i) Types of electrospraying modes of water observed during our investigation of electrospraying in combination with corona discharge.**

Only the limited number of electrospraying modes described in the literature was observed. For low flow rates (0.04 and 0.4 ml/min), with the increasing voltage applied on the spraying nozzle, the dripping mode at low voltages was followed by the spindle mode. At a short range of voltages, an oscillating spindle mode was also observed. In some cases the modes were combined with the intermittent cone-jet.

For high flow rate and long gap (4 ml/ min, 5 cm), with the increasing voltage the simple jet mode was gradually transformed into oscillating simple jet. For deionized water at a short range of voltages, a rotating simple jet mode was also observed.

Generally, for our observed modes the jets (filaments) were more elongated and disintegrated into smaller droplets for deionized water with low conductivity.

### **(ii) Effect of water with various flow rates on the electrospray with corona discharge.**

The water caused quenching effect only for high flow rates, and partially also for low flow rates. For medium flow rates, the intensive corona discharge was able to occur from the metal tips. This is an interesting and important conclusion for the water decontamination applications.

### **(iii) Effect of water conductivity on the electrospray with corona discharge.**

We observed the visible differences in the shape of water filaments (jets) and their formation in dependence of water conductivities. This effect is related to the tangential electric stress on the water filament surface. For low conductivity ( $\sim 2 \mu\text{S}/\text{cm}$ ), the jet shape was more elongated and thinner at the filament head, with higher velocity of propagation, when compared with higher conductivity ( $\sim 400 \mu\text{S}/\text{cm}$ ). Generally, the droplets with smaller sizes were formed only for low conductivity. The large acceleration values for both conductivities

(4060 m/s<sup>2</sup> and 520 m/s<sup>2</sup> for 2 μS/cm and 400 μS/cm, respectively) indicate that the process is governed by the electrostatic force.

Moreover, with the increasing conductivity, we observed the breakdown voltage reduction for corona-to-spark transition. Due to this phenomenon, the evolution of an intense streamer corona discharge was inhibited for higher conductivities.

#### **(iv) The mutual influence of discharge and the electrospray.**

The current pulses were generated by a streamer corona discharge occurring from the sharp Taylor cone tip. The generation of this discharge from the water cone depended on the repetitive process of the cone formation. After the streamer, a positive glow corona discharge was established on the water filament tip. The glow corona discharge generation and its propagation from the stressed electrode depended on the water meniscus propagation and its elongation.

Moreover, the presence of the discharge and its resultant space charge influenced the electrospray phenomenon and water filament tip curvature by disrupting the balance between the electric and the capillary forces. These phenomena were also influenced by the water conductivity; the water filament tip became more pointed with greater curvature for lower conductivity and more rounded with smaller curvature for higher conductivity. These results showed the reciprocal character of the intermittent electrospray of water and the corona discharge.

#### **(v) Potential effects of the investigated phenomena in bio-decontamination.**

From the bio-decontamination point of view we considered the intensity of corona discharge and the size of the droplets as important parameters. Owing to this consideration, we can evaluate some of the presented results.

Nozzle appears as a suitable electrode for fundamental study of electrospray with corona discharge due to the relatively stable and regular electrospray generation. However, in this configuration it is probably not suitable for bio-decontamination. Although for the low conductivity we observed relatively small droplets, the intensive discharge generation was not presented during this process. Needle is not suitable for both processes since the electrospray is irregular and unstable, and the discharge is quenched by the presence of water. Modified needle appears as a relatively suitable electrode for bio-decontamination. Although the electrospray was not always so regular and stable with small size of droplets as in the case of the nozzle, the intensive discharge generation was able to occur during this process.

For electrospraying modes observed in this study, the conductivity of water appears as important parameter determining the size of droplets. Moreover, the conductivity can influence the generation of intensive discharge. Generally, for our range of conductivities, the lower conductivity appears more suitable for bio-decontamination, due to the reduction of the size of droplets, and due to the promotion of the generation of intensive discharge.

The corona discharge (especially glow and low frequency streamers) is probably not very effective for this purpose, since we were unable to detect any biocidal reactive species such as OH radicals by OES. However we did not measure the spectra of high intensity streamer

corona discharges which can potentially lead to generation of such reactive species. This was concluded also by other works in this field.

## References

- [1] Zeleny J 1914 *Phys. Rev.* **3** 69–91
- [2] Zeleny J 1917 *Phys. Rev.* **10** 1–6
- [3] Taylor G 1964 *Proc. R. Soc. Lond. Ser. Math. Phys. Sci.* **280** 383–97
- [4] Smith D P H 1986 *IEEE Trans. Ind. Appl.* **IA-22** 527–35
- [5] Hayati I, Bailey A and Tadros T F 1987 *J. Colloid Interface Sci.* **117** 222–30
- [6] Hayati I, Bailey A I and Tadros T F 1987 *J. Colloid Interface Sci.* **117** 205–21
- [7] Bailey A G 1988 *Electrostatic Spraying of Liquids* (Taunton, Somerset, England; New York: Research Studies Press ; John Wiley & Sons)
- [8] Cloupeau M and Prunet-Foch B 1989 *J. Electrostat.* **22** 135–59
- [9] De La Mora J F and Loscertales I G 1994 *J. Fluid Mech.* **260** 155–84
- [10] Gañán-Calvo A M, Dávila J and Barrero A 1997 *J. Aerosol Sci.* **28** 249–75
- [11] Hartman R P A, Borra J-P, Brunner D J, Marijnissen J C M and Scarlett B 1999 *J. Electrostat.* **47** 143–70
- [12] Hartman R P A, Brunner D J, Camelot D M A, Marijnissen J C M and Scarlett B 2000 *J. Aerosol Sci.* **31** 65–95
- [13] Borra J-P, Ehouarn P and Boulaud D 2004 *J. Aerosol Sci.* **35** 1313–32
- [14] López-Herrera J M, Barrero A, Boucard A, Loscertales I G and Márquez M 2004 *J. Am. Soc. Mass Spectrom.* **15** 253–9
- [15] Cloupeau M and Prunet-Foch B 1994 *J. Aerosol Sci.* **25** 1021–36
- [16] Tang K and Gomez A 1996 *J. Colloid Interface Sci.* **184** 500–11
- [17] Kuroda S and Horiuchi T 1984 *Jpn. J. Appl. Phys.* **23** 1598–607
- [18] Barrero A, Gañán-Calvo A M, Dávila J, Palacios A and Gómez-González E 1999 *J. Electrostat.* **47** 13–26
- [19] Jaworek A and Krupa A 1999 *J. Aerosol Sci.* **30** 873–93
- [20] Borra J P, Tombette Y and Ehouarn P 1999 *J. Aerosol Sci.* **30** 913–25
- [21] Machala Z, Chládeková L and Pelach M 2010 *J. Phys.D: Appl. Phys.* **43** 222001

- [22] Machala Z, Tarabova B, Hensel K, Spetlikova E, Sikurova L and Lukes P 2013 *Plasma Process. Polym.* **10** 649–59
- [23] Morrow R and Lowke J J 1997 *J. Phys. D: Appl. Phys.* **30** 614–27
- [24] Morrow R 1997 *J. Phys.D: Appl. Phys.* **30** 3099–114

## Publication activities during PhD

### a) List of peer-reviewed articles

1. **B. Pongrác**, H-H. Kim, M. Janda, V. Martišovits, and Z. Machala 2014, Fast imaging of intermittent electro spraying of water with a positive corona discharge, *J. Phys. D: Appl. Phys.* – In Press  
(Impact Factor: 2.53)
2. **B. Pongrác**, H-H. Kim, N. Negishi, and Z. Machala 2014, Influence of water conductivity on particular electro spray modes with dc corona discharge – optical visualization approach, *Eur. Phys. J. D* – In Press  
(Impact Factor: 1.51)
3. H-H. Kim, Y. Teramoto, N. Negishi, A. Ogata, J-H. Kim, **B. Pongrác**, Z. Machala, and A. M. Gañán-Calvo 2014, Polarity Effect on the Electrohydrodynamic (EHD) Spray of Water, *J. Aerosol Sci.* – In Press  
(Impact Factor: 2.69)
4. **B. Pongrác**, Z. Machala 2011, Electro-Spraying of Water with Streamer Corona Discharge, *IEEE Trans. Plasma Sci.* **39**, 2664-5  
(Impact Factor: 0.87, cited: 1)
5. Z. Machala, I. Jedlovský, L. Chládeková, **B. Pongrác**, D. Giertl, M. Janda, L. Šikurová, P. Polčic 2009, DC discharges in atmospheric air for bio-decontamination – spectroscopic methods for mechanism identification, *Eur. Phys. J. D* **54**, 195-204  
(Impact Factor: 1.51, cited: 17)

### b) List of conference contributions

1. Z. Machala, K. Hensel, M. Janda, **B. Pongrác**, Z. Koval'ová, B. Tarabová, K. Tarabová, V. Martišovits, Air discharges with water, water electro spray, diagnostics and modeling, bio-medical, and environmental applications, *COST TD1208: Electrical discharges with liquids for future applications - WG4 Workshop*, Bratislava (Slovakia), October 26-31 (2013), poster

2. **B. Pongrác**, H-H. Kim, N. Negishi, and Z. Machala, Effect of Conductivity on Electro-spray of Water, *AIST internal poster conference*, Tsukuba (Japan), June 24 (2013), poster
3. **B. Pongrác**, H-H. Kim, N. Negishi, and Z. Machala, Influence of Water Conductivity on the Electro-spray with DC discharge – Optical Visualization Approach, *Joint Symposium on Plasma and Electrostatics Technologies for Environmental Applications*, Gifu (Japan), May 19-21 (2013), M20-06 p. 1-4, USB abstracts + oral presentation
4. **B. Pongrác**, V. Martišovitš, M. Janda, Z. Machala, ICCD imaging of electro-spraying of water with positive corona discharge, *IsEHD 2012: International Symposium on Electrohydrodynamics*, Gdańsk (Poland), September 23-26 (2012), p. 202-206, ISBN 978-83-934712-3-2, proceedings of IsEHD + poster
5. **B. Pongrác**, Z. Machala, Electro-spraying effect of water with corona discharge, *WDS 2011: Week of Doctoral Students: Annual Conference of Doctoral Students*, Prague (Czech Republic), May 31-June 3 (2011), poster + oral presentation
6. **B. Pongrác**, Z. Machala, V. Martišovitš, DC Discharges with Water and Their Applications, *WDS 2009: Week of Doctoral Students: Annual Conference of Doctoral Students*, Prague (Czech Republic), June 2-5 (2009), p. 101-105, ISBN 978-80-7378-102-6, proceedings of contributed papers + poster + oral presentation
7. Z. Machala, L. Chládeková, **B. Pongrác**, I. Jedlovský, L. Šikurová, Bio-Decontamination by Transient Spark and Corona Discharges with Electro-Spray, *SAPP 2009: 17th Symposium on Application of Plasma Processes*, Liptovský Ján (Slovakia), January 17-22 (2009), p. 123-124, ISBN 978-80-89186-45-7, book of contributed papers
8. Z. Machala, I. Jedlovský, **B. Pongrác**, L. Chládeková, D. Giertl, L. Šikurová, Various DC discharges for sterilization at atmospheric pressure, *HAKONE XI: 11th International Symposium on High Pressure, Low Temperature Plasma Chemistry*, Oleron (France), September 7-12 (2008), p. 530-534, contributed papers vol.2
9. Z. Machala, I. Jedlovský, D. Giertl, L. Chládeková, **B. Pongrác**, M. Zvarík, L. Šikurová, Sterilization by DC discharges at atmospheric pressure, *SPPT 2008: 23rd Symposium on Plasma Physics and Technology*, Praha (Czech Republic), June 16-19 (2008), p. 130, ISBN 978-80-01-04030-0, book of abstracts